

Switching from Ethylene Trimerization to Ethylene Polymerization by Chromium Catalysts Bearing SNS Tridentate Ligands: Process Optimization Using Response Surface Methodology

Majid Soheili¹  · Zahra Mohamadnia¹  · Babak Karimi¹ 

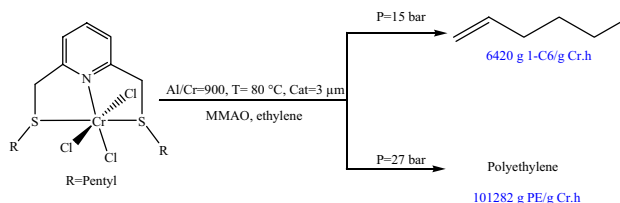
Received: 12 June 2018 / Accepted: 23 September 2018
© Springer Science+Business Media, LLC, part of Springer Nature 2018

Abstract

Two types of chromium catalysts bearing pyridine and amine based SNS ligands under the title of (pyridine-SNS-alkyl/CrCl₃) and (amine-SNS-alkyl/CrCl₃) were synthesized. Different thiolates such as octyl, pentyl, butyl, cyclohexyl and cyclopentyl thiolates were reacted with 2,6-pyridine-dimethylene-ditosylate (PMT)/THF solution at room temperature. Then, the purified pyridine-based SNS ligands (**1–5**) were reacted with CrCl₃ (THF)₃ to obtain the pyridine-SNS-alkyl/CrCl₃ catalysts (**6–10**) in 50–70% yields. MMAO-activated pyridine-SNS-alkyl/CrCl₃ catalysts were capable of oligomerizing ethylene. Statistical experimental design was conducted using the central composite design method and surface methodology to study of the effect of important parameters such as ethylene pressure, Al/Cr ratio, catalyst concentration and the reaction temperature on 1-C₆ productivity of catalyst (**7**). A quadratic polynomial equation was developed to predict the 1-C₆ productivity. Ethylene oligomerization using the catalyst (**7**) was lead to a optimized reaction conditions, including the ethylene pressure of 19.5 bar, the temperature of 58.2 °C, the MMAO co-catalyst, Al/Cr = 841 and the catalyst concentration of 8.7 μmol. The catalytic properties for ethylene oligomerization are strongly affected by reaction temperature. The experimental results indicated the reasonable agreement with the predicted values. The transformation from ethylene trimerization to ethylene polymerization of catalyst system (**7**) was occurred by exchanging the reaction pressure. Influence of ligand structure with different substitutions on sulphur atom on productivity and selectivity was investigated. 1-C₆ with the high selectivity and productivity 4318 (g 1-C₆/g Cr h) was obtained for catalyst (**7**). In the second part, 1-C₆ was obtained with high selectivity and productivity around 141 × 10³ (g 1-C₆/g Cr h) for amine-based catalyst. All amine-based catalysts (**14–16**) showed considerably higher catalytic activities compared to pyridine-based catalysts. According to the TGA analysis the thermal stability of pyridine-based catalysts was found to be higher than the amine-based catalysts.

Graphical Abstract

Chromium complexes bearing pyridine and amine based SNS ligands have been synthesized and their catalytic performance in ethylene oligomerization has been investigated. A switching from ethylene trimerization to ethylene polymerization of the catalyst (**7**) was obtained utilizing exchanging of the ethylene pressure.



Electronic supplementary material The online version of this article (<https://doi.org/10.1007/s10562-018-2571-5>) contains supplementary material, which is available to authorized users.

Extended author information available on the last page of the article

Keywords Ethylene trimerization · Chromium catalyst · 1-Hexene · Selectivity · Tridentate ligands

1 Introduction

Currently ethylene oligomerization has attracted commercial and academic media attentions affording a wide spectrum of linear α -olefins (LAOs) follow a Schulz-Flory or a Poisson type of distribution [1]. LAOs in the range of C_4 – C_{20} are the most important compounds produced by metal-catalysed ethylene oligomerization processes and used more than 3 million tons each year [2]. These valuable commodity chemicals significantly used as precursors in many areas of industry, such as detergents, plasticizer alcohols, and as co-monomer in the production of linear low density polyethylene (LLDPE) [3]. A main problem of scientists and various industries is the non-selective Schulz-Flory distribution of oligomers requiring further processes to separate the preferred products [4]. The light fraction of LAOs, such as 1-butene, especially 1-hexene, and 1-octane are mainly used for the production of LLDPE [5].

So nowadays, both industry and academia are focused on the selective processes for the production of LAOs especially 1-hexene [6]. The catalytic oligomerization of ethylene for the preparation of LAOs has increased tremendously over the last decade [7]. In the most widely used industrial processes for the preparation of LAOs such as the two-step Ziegler stoichiometric process (INEOS), one-step the Shell higher olefins process (SHOP), the Ziegler process (Chevron-Phillips Chemicals), Idemitsu and SABIC processes [8], the homogeneous catalysts are widely used. A vast number of selective ethylene trimerization catalyst based on chromium, titanium, zirconium, tantalum, and hafnium have been developed [9].

Among all of the transition metal-based oligomerization catalysts, chromium catalysts have been reported for both selective and non-selective ethylene oligomerization processes [10]. The first Cr-catalysed selective trimerization of ethylene to 1-hexene has been reported by Manyik [11]. The other chromium-based catalysts include Phillips [12], Mitsubishi [13], BP Chemicals [14], and Sasol [15]. In the past decade, several ethylene oligomerization chromium catalysts bearing N^*N^*N [16], P^*N^*P [17, 18], S^*N^*S [19–21], P^*N [22], N^*N^*P [23], N^*O^*N and N^*S^*N [24], N^*P^*N [25], P^*N^*C [26], N^*O [27], and P^*C [28], ligands have been reported and their catalytic behaviour in ethylene oligomerization have also been explored.

So in the present work, two types of novel chromium catalysts bearing pyridine and amine based SNS ligands under the titles of pyridine-SNS-alkyl/ $CrCl_3$ and amine-SNS-alkyl/ $CrCl_3$ have been prepared and evaluated as catalysts for ethylene oligomerization. The pyridine-SNS-Alkyl/ $CrCl_3$ catalysts initially developed by Gambarotta [29], and

the amine-SNS-Alkyl/ $CrCl_3$ catalysts was developed by several scientists, including McGuinness [30] and Mohamadnia [21].

Methylaluminoxane (MMAO)-activated pyridine-SNS-alkyl/ $CrCl_3$ catalysts have been tested for the ethylene oligomerization. Pyridine-SNS-alkyl/ $CrCl_3$ catalysts (Alkyl = octyl, pentyl and cyclopentyl) have not been reported yet. For the first time, the central composite method was used to design and optimization of the ethylene trimerization experiments of pyridine-SNS-pentyl/ $CrCl_3$ catalyst using response surface method (Desing-Expert® Version 7.0.0). The effects of various oligomerization conditions such as ethylene pressure, Al/Cr ratio, reaction temperature and catalyst concentration on ethylene trimerization were systematically investigated and the 1- C_6 productivity was studied as the experimental response. A literature review revealed that design and optimization of the ethylene trimerization experiments for this type of catalysts using the response surface method is novel and has not been reported previously. Ethylene oligomerization with amine-SNS-alkyl/ $CrCl_3$ catalysts were tested and compared with pyridine-SNS-alkyl/ $CrCl_3$ catalysts. Finally, 1- C_6 productivity and thermal stability of these two types of catalysts were compared.

2 Experimental

2.1 General

All reactions were carried out under an inert atmosphere of argon or nitrogen using Schlenk techniques and glovebox equipped with a purifier unit. The cocatalyst Modified Methylaluminoxane (MMAO) (7 wt% in toluene), $CrCl_3$ (THF) $_3$, 2,6-pyridinedimethanol and molecular sieve were obtained from the Aldrich (Germany). Butanethiol, 1-pentanethiol, 1-octanethiol, cyclopentanethiol, cyclohexanethiol, ethanol, THF, toluene, p-Toluenesulfonyl chloride, Na_2CO_3 , $MgSO_4$, NaCl, Na_2SO_4 , sodium and NaOH were purchased from Merck (Germany). Argon and ethylene provided by Bandar Imam Petrochemical Company (Iran) were purified by passing through NaOH, activated silica gel and molecular sieves 3 Å columns. Fourier transform infrared (FT-IR) spectroscopy was carried out by means of a Bruker Vector 22 FT-IR spectrometer (Germany) in the region of 400–4000 cm^{-1} . The samples were prepared by mixing with KBr powder in the form of pellets at ambient conditions and measured in the transmission mode. UV–Vis absorbance spectra of the samples were measured using UV/Vis spectrophotometer (Pharmacia Biothech Ultrospec 4000) and acquired between

200 and 800 nm. Thermal analysis of sample was performed by NETZSCH STA 409 PC 141H Luxx (Germany) with a heating rate of 20 K min⁻¹ under N₂ atmosphere. Temperature range was set at 25–900 °C. Prior to analysis, different samples were oven-dried at 60 °C for about 24 h. The ¹H NMR and ¹³C NMR spectra of ligands were recorded with a Bruker 400 MHz Ultrashield TM NMR instrument (Germany) at room temperature. For ¹H NMR and ¹³C NMR analysis, the samples were dissolved in CDCl₃. Elemental analysis was performed using a Vario EL III CHNOS elemental analyser. The trimerization reaction mixtures were analysed using a gas chromatograph (VARIAN CP 3800) with an FID detector.

2.2 Preparation of the Precursor 2,6-Pyridine-Dimethylene-Ditosylate (PMT)

The title compound, PMT was synthesized according to Komarsamy et al. [31] method with relatively few modifications. In a 100 mL round bottom flask (RBF) with a stir bar, NaOH (0.862 g, 21 mmol) and 2,6-pyridine dimethanol (0.3 g, 2.1 mmol) were dissolved in a mixture of THF–water (1:1) (16 mL) and the resulting solution was cooled to 0 °C. Then, *P*-toluenesulfonyl chloride (TSCI) (0.8 g, 4.2 mmol) dissolved in THF (8 mL) was added and the reaction mixture stirred for 15 min at 0 °C. Then it was stirred at room temperature for about 4 h. Water (21 mL) was added and the mixture was extracted with distilled DCM (8 mL) three times. The organic layer was washed with saturated NaCl solution (brine) to remove the bulk of the water. Then, anhydrous Na₂SO₄ drying agent was added to eliminate all traces of water. Then the organic layer was evaporated and diethyl ether was added to the residue and the crystalline precipitate was collected by filtration after cooling in a refrigerator for 3 h. It was washed with diethylether (three times) and dried under diminished pressure. PMT (white crystalline)

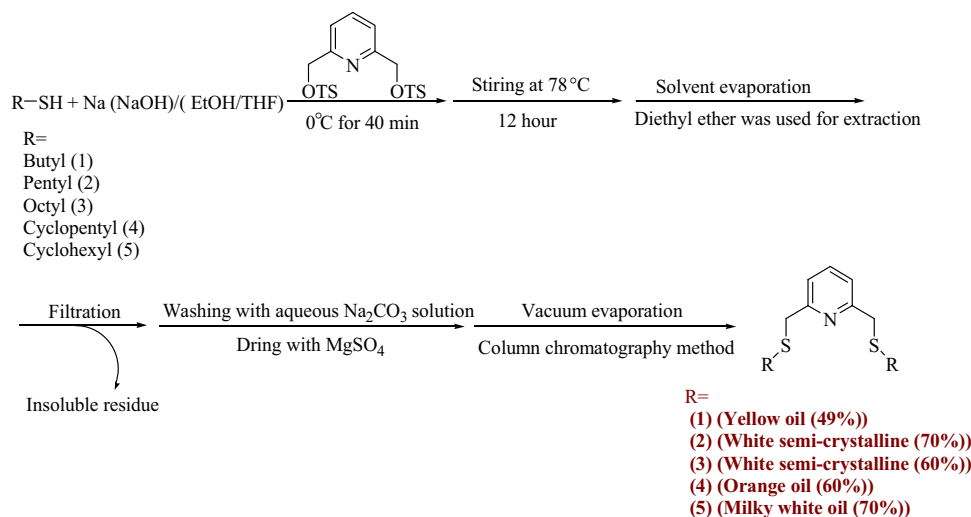
was obtained in yield of 76% and high purity (>98% pure by NMR). IR (KBr) (ν_{max} cm⁻¹): 3060 (CH_{Aromatic}), 2910 (CH_{aliphatic}), 1600, 1356, 1167 (C–O), 1065, 1032 (S=O). ¹H NMR (400 MHz, CDCl₃): δ_H 2.47 (6H, s, CH₃), 5.08 (4H, s, py-CH₂-O), 7.35 (6H, d, py and ArH), 7.73 (1H, t, py), 7.82 (4H, d, ArH). ¹³C NMR (100 MHz, CDCl₃): δ 21.7, 71.3, 121.4, 128.1, 129.9, 132.7, 137.9, 145.2, 153.5. Elemental analysis: calculated for C₂₁H₂₁NO₆S₂ (found): C 56.36(56.26), H 4.73(5.02), N 3.13(3.07), O 21.45(20.63) and S 14.33(15.02).

2.3 Preparation of the Pyridine-Based SNS Ligands (Pyridine-SNS-Alkyl) (1–5)

2.3.1 2,6-Bis(CH₃(CH₂)₃SCH₂)Pyridine (Pyridine-SNS-Butyl) (1)

Pyridine-SNS-butyl ligand was prepared according to the literature procedures with a slight modification (Scheme 1) [32]. Under argon atmosphere, butanethiol (0.406 g, 4.5 mmol) in ethanol (1 mL) was added dropwise to the stirred solution of sodium metal (0.103 g, 4.5 mmol) in ethanol (1.5 mL) at 0 °C and the solution was stirred for 40 min. The prepared mixture was added dropwise to the solution of PMT (1 g, 2.25 mmol) in ethanol and THF (1:2) (3 mL) and stirring was continued for 5 min. Then the mixture was heated under reflux overnight. The solvent was removed under vacuum and diethyl ether was added in order to remove the unreacted materials. The organic layer was washed with aqueous Na₂CO₃ (8 w/v%) followed by deionized water (2 × 30 mL), dried over anhydrous MgSO₄, filtered, concentrated under vacuum and purified using column chromatography using ethyl acetate:hexane (8:2) to give compound **1** as a yellow oil (0.31 g, 49%). IR (KBr) (ν_{max} cm⁻¹): 3060 (CH_{Aromatic}), 2927 (CH_{aliphatic}), 1589, 1573, 1454, 813, 748. ¹H NMR

Scheme 1 General procedure for synthesis of pyridine-SNS-alkyl with different R substitutions



(400 MHz, CDCl_3): δ_{H} 0.85 (6H, t, CH_3), 1.30 (4H, m, $\text{S}(\text{CH}_2)_2\text{CH}_2\text{CH}_3$), 1.50 (4H, m, $\text{SCH}_2\text{CH}_2\text{CH}_2\text{CH}_3$), 2.40 (4H, t, $\text{SCH}_2(\text{CH}_2)_2\text{CH}_3$), 3.88 (4H, s, $\text{py-CH}_2\text{S}$), 7.28 (2H, d, py), 7.63 (1H, t, py). ^{13}C NMR (100 MHz, CDCl_3): δ 13.66 ($\text{S}(\text{CH}_2)_3\text{CH}_3$), 22.17 ($\text{S}(\text{CH}_2)_2\text{CH}_2\text{CH}_3$), 29.92 ($\text{SCH}_2\text{CH}_2\text{CH}_2\text{CH}_3$), 31.27 ($\text{SCH}_2(\text{CH}_2)_2\text{CH}_3$), 38.00 ($\text{py-CH}_2\text{-S}$), 121.02 (CH-py), 137.22 (CH-py), 158.46 (C-py). Elemental analysis: calculated for $\text{C}_{15}\text{H}_{25}\text{NS}_2$ (found): C 63.55(63.44), H 8.89(8.92), N 4.94(5.13), and S 22.62(22.51).

2.3.2 2,6-Bis($\text{CH}_3(\text{CH}_2)_4\text{SCH}_2$)Pyridine (Pyridine-SNS-Pentyl) (2)

Pyridine-based ligand with pentyl substituent (2) was synthesized according to the method 1 with the following molar ratio of starting materials, pentanethiol (0.62 g, 6 mmol), sodium (0.138 g, 6 mmol), PMT (1.34 g, 3 mmol) to give compound 2 as a white semi-crystalline solid (0.1 g, 70%). IR (KBr) (ν_{max} cm^{-1}): 3050 ($\text{CH}_{\text{Aromatic}}$), 2924 ($\text{CH}_{\text{aliphatic}}$), 1589, 1573, 1454, 820, 748. ^1H NMR (400 MHz, CDCl_3): δ_{H} 0.88 (6H, t, $\text{S}(\text{CH}_2)_4\text{CH}_3$), 1.2–1.50 (8H, m, $\text{S}(\text{CH}_2)_2(\text{CH}_2)_2\text{CH}_3$), 1.6–1.8 (4H, m, $\text{SCH}_2\text{CH}_2(\text{CH}_2)_2\text{CH}_3$), 2.58 (4H, t, $\text{SCH}_2(\text{CH}_2)_3\text{CH}_3$), 4.16 (4H, s, $\text{py-CH}_2\text{-S}$), 7.57 (2H, d, py), 7.98 (1H, t, py). ^{13}C NMR (100 MHz, CDCl_3): δ 13.97 ($\text{S}(\text{CH}_2)_4\text{CH}_3$), 22.25 ($\text{S}(\text{CH}_2)_3\text{CH}_2\text{CH}_3$), 28.89 ($\text{S}(\text{CH}_2)_2\text{CH}_2\text{CH}_2\text{CH}_3$), 30.94 ($\text{SCH}_2\text{CH}_2(\text{CH}_2)_2\text{CH}_3$), 32.29 ($\text{SCH}_2(\text{CH}_2)_3\text{CH}_3$), 34.89 ($\text{py-CH}_2\text{-S}$), 123.19 (CH-py), 141.41 (CH-py), 157.07 (C-py). Elemental analysis: calculated for $\text{C}_{17}\text{H}_{29}\text{NS}_2$ (found): C 65.54(65.24) H 9.38(9.44) N 4.50(4.90) and S 20.58(20.42).

2.3.3 2,6-Bis($\text{CH}_3(\text{CH}_2)_7\text{SCH}_2$)Pyridine (Pyridine-SNS-Octyl) (3)

According to the procedure 1, a white semi-crystalline compound (3) (yield: 60%) was synthesized. IR (KBr) (ν_{max} cm^{-1}): 3065 ($\text{CH}_{\text{Aromatic}}$), 2921 ($\text{CH}_{\text{aliphatic}}$), 1584, 1465, 820. ^1H NMR (400 MHz, CDCl_3): δ_{H} 0.89 (6H, t, CH_3), 1.1–1.50 (20H, m, $\text{S}(\text{CH}_2)_2(\text{CH}_2)_5\text{CH}_3$), 1.6–1.8 (4H, m, $\text{SCH}_2\text{CH}_2(\text{CH}_2)_5\text{CH}_3$), 2.5 (4H, t, $\text{SCH}_2\text{CH}_2(\text{CH}_2)_5\text{CH}_3$), 3.84 (4H, s, $\text{py-CH}_2\text{-S}$), 7.3 (2H, d, py), 7.64 (1H, t, py). ^{13}C NMR (100 MHz, CDCl_3): δ 14.01 ($\text{S}(\text{CH}_2)_7\text{CH}_3$), 22.6 ($\text{S}(\text{CH}_2)_6\text{CH}_2\text{CH}_3$), 28.90 ($\text{S}(\text{CH}_2)_5\text{CH}_2\text{CH}_2\text{CH}_3$), 29.20 ($\text{S}(\text{CH}_2)_3(\text{CH}_2)_2(\text{CH}_2)_2\text{CH}_3$), 29.30 ($\text{S}(\text{CH}_2)_2\text{CH}_2(\text{CH}_2)_4\text{CH}_3$), 31.70 ($\text{SCH}_2\text{CH}_2(\text{CH}_2)_5\text{CH}_3$), 31.80 ($\text{SCH}_2(\text{CH}_2)_6\text{CH}_3$), 38.10 ($\text{py-CH}_2\text{-S}$), 121.10 (CH-py), 137.30 (CH-py), 158.50 (C-py). Elemental analysis: calculated for $\text{C}_{23}\text{H}_{41}\text{NS}_2$ (found): C 69.81(70.11), H 10.44(10.49), N 3.54(3.35) and S 16.21(16.05).

2.3.4 2,6-Bis($(\text{CH}_2)_4\text{CHSCH}_2$)Pyridine (Pyridine-SNS-Cyclopentyl) (4)

The title ligand (4) was synthesized according to the method reported by Temple et al. [29] with some modifications (Scheme 1). Under argon atmosphere, a solution of cyclopentanethiol (0.46 g, 4.5 mmol) in ethanol (5 mL) was added dropwise to a solution of sodium hydroxide (0.18 g, 4.5 mmol) in ethanol (7.5 mL) and stirred for 40 min. Then it was added dropwise to the solution of PMT (1 g, 2.25 mmol) in THF (12 mL). After 24 h stirring at room temperature, the solvent was removed under vacuum and the residue was twice extracted to remove unreacted materials by adding DCM/deionized water (1:1) (8 mL). The combined aqueous layers were washed with DCM (3 \times 20 mL), and the combined organic layers were dried over anhydrous MgSO_4 , concentrated and purified using column chromatography to give an orange oil (4) (0.39 g, 60%). IR (KBr) (ν_{max} cm^{-1}): 3085 ($\text{CH}_{\text{Aromatic}}$), 2954 ($\text{CH}_{\text{aliphatic}}$), 1590, 1572, 1451, 813, 703. ^1H NMR (400 MHz, CDCl_3): δ_{H} 1.4–1.6 (8H, m, $\text{SCH}(\text{CH}_2)_2(\text{CH}_2)_2$), 1.95–2.1 (8H, m, $\text{SCH}(\text{CH}_2)_2(\text{CH}_2)_2$), 3–3.2 (2H, m, $\text{SCH}(\text{CH}_2)_4$), 3.87 (4H, s, $\text{py-CH}_2\text{-S}$), 7.27 (2H, d, py), 7.62 (1H, t, py). ^{13}C NMR (100 MHz, CDCl_3): δ 24.89 $\text{SCH}(\text{CH}_2)_2(\text{CH}_2)_2$, 33.68 $\text{SCH}(\text{CH}_2)_2(\text{CH}_2)_2$, 38.37 $\text{SCH}(\text{CH}_2)_4$, 43.56 ($\text{py-CH}_2\text{-S}$), 121.01 (CH-py), 137.18 (CH-py), 158.57 (C-py). Elemental analysis: calculated for $\text{C}_{17}\text{H}_{25}\text{NS}_2$ (found): C 66.40(65.77), H 8.19(10.49), N 4.55(4.05) and S 20.85(19.69).

2.3.5 2,6-bis($(\text{CH}_2)_5\text{CHSCH}_2$)Pyridine (Pyridine-SNS-Cyclohexyl) (5)

According to the procedure for preparation of 4, a milky-white oil (5) (yield: 70%) was synthesized. IR (KBr) (ν_{max} cm^{-1}): 3058 ($\text{CH}_{\text{Aromatic}}$), 2854 ($\text{CH}_{\text{aliphatic}}$), 1588, 1572, 1449, 814, 704. ^1H NMR (400 MHz, CDCl_3): δ_{H} 1.1–1.4 (4H, m, $\text{SCH}(\text{CH}_2)_4\text{CH}_2$), 1.6–1.8 (8H, m, $\text{SCH}(\text{CH}_2)_2(\text{CH}_2)_2\text{CH}_2$), 1.9–2.0 (8H, m, $\text{SCH}(\text{CH}_2)_2(\text{CH}_2)_3$), 2.55–2.7 (2H, m, $\text{SCH}(\text{CH}_2)_5$), 3.86 (4H, s, $\text{py-CH}_2\text{-S}$), 7.27 (2H, d, py), 7.61 (1H, t, py). ^{13}C NMR (100 MHz, CDCl_3): δ 25.84 $\text{SCH}(\text{CH}_2)_4\text{CH}_2$, 26.02 $\text{SCH}(\text{CH}_2)_2(\text{CH}_2)_2\text{CH}_2$, 33.43 $\text{SCH}(\text{CH}_2)_2(\text{CH}_2)_3$, 36.55 $\text{SCH}(\text{CH}_2)_5$, 43.32 ($\text{py-CH}_2\text{-S}$), 120.89 (CH-py), 137.20 (CH-py), 158.72 (C-py). Elemental analysis: calculated for $\text{C}_{19}\text{H}_{29}\text{NS}_2$ (found): C 68.00(66.28), H 8.71(10.79), N 4.17(3.84), and S 19.11 (19.09).

2.4 General Procedure for the Synthesis of 2,6-Bis(Alkyl SCH_2)Pyridine/ CrCl_3 Catalysts (Pyridine-SNS-Alkyl/ CrCl_3) (6–10)

All pyridine-SNS-alkyl/ CrCl_3 catalysts were synthesized according to the method reported by Sandro Gambarotta et al. [29] $\text{CrCl}_3(\text{THF})_3$ (0.12 mmol) was added to a solution

of pyridine-SNS-alkyl ligands (0.126 mmol) in dry toluene (5 mL) at room temperature and stirred for 40 min (Scheme S1). A visible colour change to green was observed. The catalyst was recovered by centrifuging and decantation of the reaction mixture. It was then washed with *n*-hexane (3 × 5 mL) and dried under vacuum.

2.4.1 Pyridine-SNS-Butyl/CrCl₃ (6)

The catalyst (**6**) was green solid with 61% yield. IR (KBr) (ν_{\max} cm⁻¹): 3100 (CH_{aromatic}), 2900 (CH_{aliphatic}), 1603, 1577, 1459, 889, 794. Elemental analysis calculated for C₁₅H₂₅Cl₃CrNS₂ (found): C 40.78(41.10), H 5.70(5.91), N 3.17(2.97), S 14.51(14.34), Cl 24.07 (–), and Cr 11.77 (–).

2.4.2 Pyridine-SNS-Pentyl/CrCl₃ (7)

The catalyst (**7**) was green solid with 70% yield. IR (KBr) (ν_{\max} cm⁻¹): 3040 (CH_{aromatic}), 2906 (CH_{aliphatic}), 1603, 1568, 1460, 884, 797. Elemental analysis calculated for C₁₇H₂₉Cl₃CrNS₂ (found): C 43.45(43.27), H 6.22(6.87), N 2.98(2.74), S 13.65(13.60), Cl 22.63 (–), and Cr 11.07 (–).

2.4.3 Pyridine-SNS-Octyl/CrCl₃ (8)

The catalyst (**8**) was green solid with 70% yield. IR (KBr) (ν_{\max} cm⁻¹): 3035 (CH_{aromatic}), 2858 (CH_{aliphatic}), 1601, 1569, 1463, 895, 815. Elemental analysis calculated for C₂₃H₄₁Cl₃CrNS₂ (found): C 49.86(49.49), H 7.46(7.73), N 2.53(2.40), S 11.57(12.09), Cl 19.19 (–), and Cr 9.38 (–).

2.4.4 Pyridine-SNS-Cyclopentyl/CrCl₃ (9)

The catalyst (**9**) was green solid with 63% yield. IR (KBr) (ν_{\max} cm⁻¹): 3035 (CH_{aromatic}), 2913 (CH_{aliphatic}), 1602, 1569, 1453, 794, 733. Elemental analysis calculated for C₁₇H₂₅Cl₃CrNS₂ (found): C 43.83(44.22), H 5.41(5.82), N 3.01(2.94), S 13.76(13.30), Cl 22.83 (–), and Cr 11.16 (–).

2.4.5 Pyridine-SNS-Cyclohexyl/CrCl₃ (10)

The catalyst (**10**) was green solid with 51% yield. IR (KBr) (ν_{\max} cm⁻¹): 3035 (CH_{aromatic}), 2912 (CH_{aliphatic}), 1608, 1570, 1462, 1034, 1032. Elemental analysis calculated for C₁₉H₂₉Cl₃CrNS₂ (found): C 46.20 (46.51), H 5.92(6.08), N 2.84(2.77), S 12.98(12.58), Cl 21.53 (–), and Cr 10.53 (–).

2.5 General Procedure for Synthesis of Amine-SNS-Alkyl Ligands (11–13)

All amine-based SNS ligands were synthesized according to our previous methods [19, 21]. A solution of NaOH (25 mmol) and thiol (25 mmol) in ethanol (25 mL) was

added to the stirred solution of bis(2-chloroethyl)amine hydrochloride (8.33 mmol) in ethanol (16 mL) at 0 °C. After stirring at 0 °C for 2 h followed by room temperature for 16 h, the mixture was filtered, the filtrate evaporated using rotary evaporator, the residue taken up with dry *n*-hexane and diethyl ether respectively and filtered again. Finally, the solvent was evaporated under vacuum to give the amine-based ligands.

2.5.1 Bis-(2-Butylsulfanyl-Ethyl)-Amine Ligand (Amine-SNS-Butyl) (11)

Ligand (**11**) was colorless oil with 74% yield. IR (KBr) (ν_{\max} cm⁻¹): 3305 (NH), 2960 (CH_{aliphatic}), 1465, 1301, 765. ¹H NMR (400 MHz, CDCl₃): δ_{H} 0.93 (6H, t, CH₃), 1.38–1.52 (4H, m, SC₂H₄CH₂CH₃), 1.55–1.61 (4H, m, SCH₂CH₂C₂H₅), 1.90 (1H, broad, NH), 2.30 (4H, t, SCH₂C₃H₇), 2.57 (4H, t, SCH₂CH₂NH), 2.71 (4H, t, NHCH₂). ¹³C NMR (100 MHz, CDCl₃): δ 13.66 (CH₃), 21.60 (SC₂H₄CH₂CH₃), 31.63 (SCH₂CH₂C₂H₅), 31.80 (SCH₂C₃H₇), 32.29 (SCH₂CH₂NH), 48.30 (SCH₂CH₂NH). Elemental analysis: calculated for C₁₂H₂₇NS₂ (found): C 57.77 (58.46), H 10.91 (12.15), N 5.61 (6.12) and S 25.71 (23.27).

2.5.2 Bis-(2-octylsulfanyl-ethyl)-amine ligand (Amine-SNS-Octyl) (12)

Amine-based SNS ligand with octyl substitution (**12**) was colourless oil with 74% yield. IR (KBr) (ν_{\max} cm⁻¹): 3283 (NH), 2928(CH_{aliphatic}), 1450, 1370, 1290, 717. ¹H NMR (400 MHz, CDCl₃): δ_{H} 0.90 (6H, t, CH₃), 1.21–1.40 (16H, m, S(CH₂)₃C₄H₈CH₃), 1.54–1.63 (4H, m, SC₂H₄CH₂C₅H₁₀), 1.64–1.74 (4H, m, SCH₂CH₂C₆H₁₂), 1.85 (1H, broad, NH), 2.51 (4H, t, SCH₂C₇H₁₄), 2.68 (4H, t, SCH₂CH₂NH), 2.84 (4H, t, NHCH₂). ¹³C NMR (100 MHz, CDCl₃): δ 14.22 (S(CH₂)₇CH₃), 22.56 (S(CH₂)₆CH₂CH₃), 28.0 (C₅H₁₀CH₂C₂H₅), 29.21 (S(CH₂)₄CH₂(CH₂)₂CH₃), 29.79 (S(CH₂)₃CH₂(CH₂)₃CH₃), 31.82 (S(CH₂)₂CH₂(CH₂)₄CH₃), 32.06 (SCH₂CH₂(CH₂)₅CH₃), 32.35 (SCH₂(CH₂)₆CH₃), 39.27 (SCH₂CH₂NH), 48.37 (SCH₂CH₂NH). Elemental analysis: calculated for C₂₀H₄₃NS₂ (found): C 66.42 (65.47), H 11.98 (12.18), N 3.87 (4.82) and S 17.73 (17.53).

2.5.3 Bis-(2-Cyclopentylsulfanyl-Ethyl)-Amine Ligand (Amine-SNS-Cyclopentyl) (13)

Ligand (**13**) was colorless oil with 60% yield. IR (KBr) (ν_{\max} cm⁻¹): 3299 (NH), 2954(CH_{aliphatic}), 1750, (N-H), 1450, 1124, 735. ¹H NMR (400 MHz, CDCl₃): δ_{H} 1.36–1.56 (8H, m, SCH(CH₂)₂(CH₂)₂), 1.84–1.94 (8H, m, SCH(CH₂)₂(CH₂)₂), 2.00 (1H, broad, NH), 2.62 (4H, t, SCH₂CH₂NH), 2.76 (4H, t, NHCH₂), 2.98–3.05 (2H,

m, SCH(CH₂)₂(CH₂)₂). ¹³C NMR (100 MHz, CDCl₃): δ 24.72 (SCHC₂H₄C₂H₄), 31.98 (SCHC₂H₄C₂H₄), 33.90 (SCHC₂H₄C₂H₄), 43.68 (SCH₂CH₂NH), 48.54 (SCH₂CH₂NH). Elemental analysis: calculated for C₁₄H₂₇NS₂ (found): C 61.48 (60.72), H 9.95 (9.60), N 5.12 (6.86) and S 23.44 (22.82).

2.6 General Procedure for Synthesis of Amine-SNS-Alkyl/CrCl₃ Catalysts (14–16)

All amine-SNS-Alkyl/CrCl₃ catalysts were prepared according to our previous methods [19, 21]. The prepared ligands (0.235 mmol) in THF (5 mL) was added dropwise to a stirred solution of CrCl₃(THF)₃ (0.215 mmol) in THF (5 mL) at room temperature and the solution kept under stirring for 10 min. Then the solvent was removed in vacuum, diethyl ether (10 mL) added to the solid residue, cooled overnight in a refrigerator, centrifuged, washed with diethyl ether (3 × 10 mL), and dried under vacuum.

2.6.1 Amine-SNS-Butyl/CrCl₃ (14)

The catalyst (**14**) was blue-green solid with 58% yield. Elemental analysis: calculated for C₁₂H₂₇Cl₃CrNS₂ (found): C 35.34 (35.02), H 6.67 (7.0), N 3.43 (3.75), S 15.72 (15.40), Cl 26.08 (–), and Cr 12.75 (–).

2.6.2 Amine-SNS-Octyl/CrCl₃ (15)

The catalyst (**15**) was green solid with 54% yield. Elemental analysis: calculated for C₂₀H₄₃Cl₃CrNS₂ (found): C 46.19 (45.25), H 8.33 (8.08), N 2.69 (2.84), S 12.33 (13.38), Cl 20.45 (–), and Cr 10.00 (–).

2.6.3 Amine-SNS-Cyclopentyl/CrCl₃ (16)

The catalyst (**16**) was green solid with 64% yield. Elemental analysis: calculated for C₁₄H₂₇Cl₃CrNS₂ (found): C 38.94 (38.83), H 6.30 (7.02), N 3.24 (3.45), S 14.85 (14.30), Cl 24.63 (–), and Cr 12.04 (–).

2.7 Catalytic Ethylene Oligomerization

The catalytic ethylene oligomerization reactions were performed in a stainless steel research reactor. The high pressure reactor was temperature and pressure controlled. Before each run, the reactor was dried in an oven at 130 °C for 3 h, vacuumed for 30 min and purged with three cycles of argon/vacuum. The reactor was then preheated, charged with toluene and the desired amount of MMAO, pressurized with ethylene, and stirred at the considered reaction temperature. After 10 min, equilibrium has been reached. At that time, a specific volume of the catalyst solution in toluene was

injected into the reactor to start the ethylene oligomerization. The reaction temperature and ethylene pressure were kept constant during the reaction. The mixture was stirred for 30 min. The reactor was then cooled to –10 °C. The liquid phase was analysed by GC and solid polyethylene collected by filtration, washed with MeOH, dried, and weighed.

2.7.1 Study of Catalytic Ethylene Oligomerization Using Response Surface Methodology

Based on our previous studies, four parameters including ethylene pressure, Al/Cr ratio, reaction temperature and catalyst concentration were identified as the key factors affecting the 1-C₆ productivity. For the first time, response surface methodology (RSM) was employed to investigate the effect of the independent variables; ethylene pressure, Al/Cr ratio, reaction temperature and catalyst concentration. The experiments were analysed using central composite design (CCD). Design matrix was generated and results were statistically analysed using Design Expert version 7.0.0 by Stat-Ease Inc. (Minneapolis, USA). The center of the experimental field was performed 5 times for CCD. Each design was evaluated separately based on the influence of variables on 1-hexene productivity (g 1-C₆/g Cr h). The design was expressed by polynomial regression equation to generate the model. The model quality and significance of various factors considering the sum of squares and residual sum of squares were estimated by analysis of variance (ANOVA). The analysis included the F test, related probability values, coefficient of determination R² which measures the goodness of fit of regression model. The experimental and predicted developed results were compared in order to approve the validity of the model.

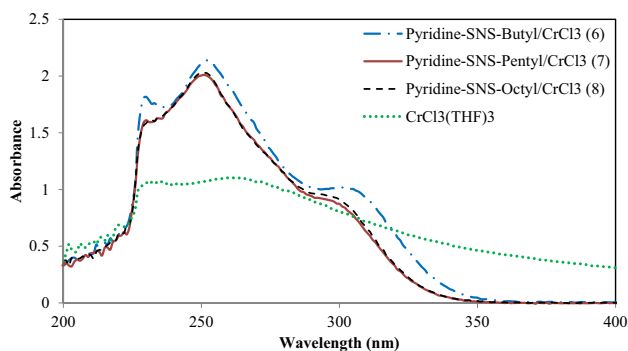
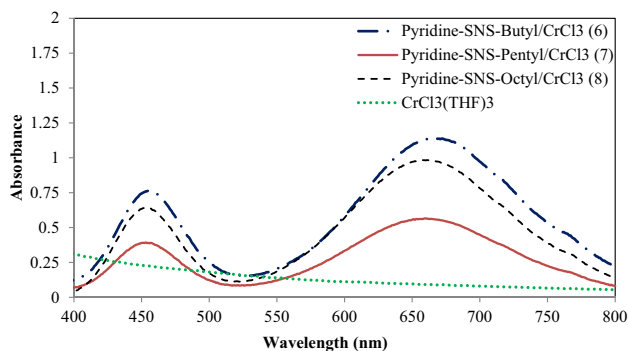
3 Results and Discussion

3.1 FT-IR Analysis of Pyridine-Based Ligands and Their Corresponding Catalysts

Table 1 shows a summary of the most important bands in the FT-IR spectra which correspond to the –C=N stretching (1580–1600 cm^{–1}), the C=C stretching aromatic (1500–1600 cm^{–1}), C–S stretching (600–800 cm^{–1}) and C–H bending vibrations. Significant shifts in vibration frequencies, such as increasing of the C=N stretching frequency of **6** from 1589 to 1603 cm^{–1} and C–S stretching frequency of **8** from 802 to 815 cm^{–1}, are interpreted as signs of successful complexation of the pyridine-based SNS ligands to the chromium center. There was no clear difference between the vibration frequencies of the other ligands such as C=C stretching and C–H bending for ligands and their corresponding catalysts.

Table 1 Comparison between the important vibration frequencies of the ligands and their corresponding catalysts

Ligand/complex	FT-IR $\nu_{\max}/\text{cm}^{-1}$			
	C=N	C=C	C-S	C-H
Pyridine-SNS-butyl (1)	1589	1573	748	1454
Pyridine-SNS-butyl/CrCl ₃ (6)	1603	1577	794	1459
Pyridine-SNS-octyl (3)	1584	1584	802	1465
Pyridine-SNS-octyl/CrCl ₃ (8)	1601	1569	815	1463
Pyridine-SNS-cyclopentyl (4)	1590	1572	703	1451
Pyridine-SNS-cyclopentyl/CrCl ₃ (9)	1602	1569	733	1453

**Fig. 1** Comparison between UV-Vis absorption spectra of CrCl₃(THF)₃ and pyridine-SNS-alkyl/CrCl₃ catalysts (UV region)**Fig. 2** Comparison between UV-Vis absorption spectra of CrCl₃(THF)₃ with the pyridine-SNS-alkyl/CrCl₃ catalysts (visible region)**Table 2** Experimental values of the d-d transitions for the ethylene trimerization chromium site

Compounds name	Chromophore	⁴ A _{2g} (F)→ ⁴ T _{1g} (P)	⁴ A _{2g} (F)→ ⁴ T _{1g} (F)	⁴ A _{2g} (F)→ ⁴ T _{2g} (F)
		(ν_1)	(ν_2)	(ν_3)
nm				
CrCl ₃ (THF) ₃	CrO ₃ Cl ₃	–	–	–
Pyridine-SNS-butyl/CrCl ₃ (6)	CrNS ₂ Cl ₃	450	670	–
Pyridine-SNS-pentyl/CrCl ₃ (7)	CrNS ₂ Cl ₃	449	659	–
Pyridine-SNS-octyl/CrCl ₃ (8)	CrNS ₂ Cl ₃	449	652	–

3.2 UV-Visible Spectra of Pyridine-Based Catalysts

The UV-Visible absorption spectra of the catalysts displayed meridional coordination of the pyridine-based SNS ligands (Figs. 1, 2) [33]. As shown in Fig. 1, absorptions in the ultraviolet region are related to π to π^* and ligand to metal transitions. In visible region, octahedral pyridine-based complexes with d^3 electron configuration show three spin-allowed transitions (Fig. 2). According to the Russell-Saunders coupling, in octahedral fields, F and P terms split into crystal field components ($A_{2g}(F)$, $T_{2g}(F)$, $T_{1g}(F)$ and $T_{1g}(P)$) having different energies. The pyridine-based catalysts consist of a regular octahedron CrNS_2Cl_3 containing Cr^{III} , which gives rise to two distinct d-d transitions at ~ 450 nm (ν_1 : ${}^4A_{2g}(F) \rightarrow {}^4T_{1g}(P)$) and ~ 650 nm (ν_2 : ${}^4A_{2g}(F) \rightarrow {}^4T_{1g}(F)$). The third allowed d-d transition (ν_3 : ${}^4A_{2g}(F) \rightarrow {}^4T_{2g}(F)$) almost is placed in visible region (Table 2).

3.3 Evaluation of Thermal Stability of Pyridine-Based Catalysts

The thermogravimetric analysis (TGA) curves in nitrogen atmosphere showed that the pyridine-based complexes display high thermal stability (Fig. S1). The decomposition temperatures (T_{dec}) for 5% weight loss were observed in the range of 210 °C for compound 7 [34]. During the heating process, there is a multi-stage weight loss without formation of steady interfaces. Due to the lower binding energy of C-S bond, the possibility of the catalyst cleavage is increased from this position. Table 3 shows the comparison between experimental and theoretical weight loss percent for various fragments of catalyst (7). The initial weight loss ($\sim 3.9\%$) is related to the residual organic solvent and water. The presence of water molecules has been already seen in the FT-IR spectra of the catalyst (7). The second and the third weight loss ($\sim 43.77\%$) in the temperature range of 120–380 °C, presumably due to loss of the SC_5H_{11} fragment of the SNS ligand. The fourth weight loss (6%) in the temperature range of 480–480 °C is related to the dissociation of the methylene. The final weight loss (5.86%) in the temperature range of 640–800 °C is attributed to the degradation of the C_3H_3 fragment of the pyridine ring. The residual mass above

Table 3 Comparison between experimental and theoretical weight loss percent for various fragments of catalyst (7)

Segments	Molar masses of the fragments (g/mol)	Temperature (°C)	Weight loss % (Theoretical)	Weight loss % (Experimental)
2 × (SC ₅ H ₁₁)	206	120–380	44	43.8
2 × (CH ₂)	28	380–460	5.98	6
C ₃ H ₃ (pyridine)	39	640–800	7.7	5.9
CrCl ₃ NC ₂	195	Above 800	41.8	40.5

800 °C can be assigned to the sum of the residual pyridine fragment of the ligand with CrCl₃.

3.4 Catalytic Ethylene Oligomerization Using Pyridine-SNS-Pentyl/CrCl₃ Catalyst (7)

An ethylene trimerization reaction using the pyridine-based catalysts activated by MMAO co-catalyst, afforded 99% 1-C₆. Transition metal-based oligomerization catalysts generally not able to produce alpha-olefin alone and must be activated by appropriate co-catalysts. Among the important co-catalysts, perfluoroaryl boranes, fluoroarylanes, trityl, aluminum alkyls and methylaluminumoxane (MAO) are mentioned. It is generally accepted that the cocatalyst, among other functions such as removal the water and oxygen contaminant and easily reduction of chromium, facilitates alkyl abstraction from the catalyst precursor to yield an anionic

cocatalyst fragment [RX⁻] and a cationic metal fragment [L_nM⁺], which in combination represents the active catalytic system as an ion pair represented by [L_nM⁺][RX⁻] [25, 35].

According to the preliminary tests, our focus is on 1-C₆ production with catalyst (7) only and the various factors which could affect the catalytic activity including Al/Cr ratio, catalyst concentration (μmol), ethylene pressure (bar), reaction temperature, were investigated using the surface response methodology (RSM) based on the CCD design in order to reach the maximum 1-C₆ production (Table 4). Moreover, the effect of different R groups on the 1-C₆ productivity was examined. 1-C₆ as a main product and other by-products such as 1-octane and 1-decene in the liquid fraction were measured by gas chromatography (GC). In Table 5, the factors and their levels are shown to achieve the optimum conditions for the catalyst activity based on the

Table 4 Experimental design layout for ethylene oligomerization and the obtained results

Run	A: Al/Cr	B: Catalyst (μmol)	C: Ethylene pressure (bar)	D: Temperature (°C)	1-C ₆ productivity (g 1-C ₆ /g Cr h)	PE (g)
1	700	6	21	52.5	2090	0.15
2	700	6	21	52.5	1537	0.13
3	700	6	21	52.5	1537	0.13
4	700	6	21	52.5	1537	0.13
5	700	6	21	52.5	2070	0.13
6	900	9	27	25	1200	–
7	900	9	15	25	130	–
8	900	3	27	80	350	7.9
9	500	9	15	80	169	0.25
10	900	3	15	80	6420	0.021
11	500	3	27	25	817	0.1
12	500	9	27	80	934	0.14
13	500	3	15	25	311	0.11
14	500	6	27	52.5	4318	0.14
15	900	6	21	52.5	4084	0.1
16	700	3	21	52.5	1167	0.12
17	700	9	21	52.5	4020	0.08
18	700	6	15	52.5	3404	0.07
19	700	6	27	52.5	5330	0.1
20	700	6	21	25	14	0.1
21	700	6	21	80	5135	0.08

Table 5 Factors and levels according to response surface model

Factor	Name	Units	Low actual	High actual	Low coded	High coded	Mean	Std. dev.
A	Al/Cr	–	500	900	– 1	1	700	138.013
B	Catalyst	μmol	3	9	– 1	1	6	2.070
C	Pressure	Bar	15	27	– 1	1	21	4.140
D	Temperature	°C	25	80	– 1	1	52.5	18.977
Response	Name	Units	Analysis	Minimum	Maximum	Mean	Std. dev.	
Y	1-C ₆ productivity	g 1-C ₆ /g Cr h	Polynomial	14	6420	2217.81	1903.88	

RSM. The variables A, B, C and D, respectively, indicate the Al/Cr ratio, the catalyst concentration, the ethylene pressure, and the reaction temperature.

Some factors in the analysis of variance (ANOVA) table such as coefficient of determination (R²), adjusted R², lack of fitness and P-value are important for selection of adequate models. The significance of the lack of fitness for a model indicates that the points are not well positioned around the model and that the model cannot be used to predict the values of the dependent variables. So the data was fitted with various models and their subsequent ANOVA showed that 1-C₆ productivity was most suitably defined by quadratic polynomial model. The final model to predict the 1-C₆ productivity of catalyst **7** is shown in Eq. (1):

$$\begin{aligned} \ln(\text{productivity } 1\text{-C}_6) = & +7.65 - 0.028A + 0.62B + 0.24C \\ & + 2.95D + 2.68AB - 0.42AC \\ & + 1.01AD + 0.73BC - 0.30BD \\ & - 0.55CD + 0.54A^2 - 0.12B^2 \\ & + 0.56C^2 - 2.21D^2 \end{aligned} \quad (1)$$

As shown in ANOVA Table 6, the lack of fit numbers for all parameters, which measure the fitness of the model, were not significant (<0.05) and high model F-value (39.52) further confirmed the reliability of the models within the considered range of process conditions. The R² value (R-squared) close to 1, shows the greater ability of the model to predict a trend. Normally, a regression model with an R² higher than 0.90, is considered to have

Table 6 Analysis of variance (ANOVA) according to response surface quadratic model for the response of 1-C₆ productivity using catalyst (7)

Source	Sum of squares	df	Mean square	F value	p-value Prob > F	Remark
Model						
R ² : 0.99						
Adj R ² : 0.96	45.261	14	3.233	39.526	<0.0001	Significant
A: Al/Cr	0.001	1	0.001	0.019	0.8949	
B: Catalyst	0.765	1	0.765	9.351	0.0223	Significant
C: Pressure	0.594	1	0.594	7.262	0.0358	Significant
D: Temperature	17.433	1	17.433	213.136	<0.0001	Significant
AB	11.479	1	11.479	140.336	<0.0001	Significant
AC	1.413	1	1.413	17.275	0.0060	Significant
AD	1.636	1	1.636	20.008	0.0042	Significant
BC	4.315	1	4.315	52.751	0.0003	Significant
BD	0.143	1	0.143	1.747	0.2344	
CD	2.407	1	2.407	29.426	0.0016	Significant
A ²	0.750	1	0.750	9.163	0.0232	Significant
B ²	0.037	1	0.037	0.451	0.5268	
C ²	0.790	1	0.790	9.651	0.0209	Significant
D ²	12.461	1	12.461	152.352	<0.0001	Significant
Residual	0.491	6	0.082			
Lack of fit	0.381	2	0.190	6.933	0.0501	Not significant
Pure error	0.110	4	0.027			
Correlation total	45.752	20				

a very high association [36]. The R^2 of 0.99 is in reasonable agreement with the “adj R^2 ” of 0.96. The “adj R^2 ” value corrects the R^2 value for the 1- C_6 productivity and for the number of terms in the model. A high value of the adjusted R-squared (adj $R^2=0.9642$) promotes for a high significance of the model.

The influence and importance of the variable can be shown by the sign and their coefficients. Therefore, the negative sign of variable A (Al/Cr) indicates its opposite effect on the 1- C_6 productivity parameter. This is while the positive sign of the coefficient of variable B (catalyst concentration), C (gas pressure ethylene) and D (temperature) indicate their direct correlation with the response. The value of the coefficient D (2.95) is greater than the coefficients A, C and B indicating the greater importance of temperature on the catalyst productivity in ethylene trimerization, while Al/Cr with a coefficient of -0.028 has the least effect on activity.

The significance of each coefficient in Eq. 1 was checked using F-test. Values of “Prob > F” less than 0.05 indicates that the model terms are significant. In this case B, C, D, AB, AC, AD, BC, CD, A^2 , C^2 and D^2 are the model significant terms. In order to improve the model, the non-significant coefficients were excluded and the final model was developed as Eq. (2):

$$\begin{aligned} \ln(\text{productivity } 1\text{-}C_6) = & +7.65 + 0.62B + 0.24C + 2.95D \\ & + 2.68AB - 0.42AC + 1.01AD \\ & + 0.73BC - 0.55CD + 0.54A^2 \\ & + 0.56C^2 - 2.21D^2 \end{aligned} \quad (2)$$

The interaction between factors also was investigated by using the response surface methodology (RSM). According to Fig. 3a, when the Al/Cr ratio is proportional to the catalyst concentration, the productivity of 1- C_6 is high (e.g., Al/Cr = 900 and 9 μm catalyst or Al/Cr = 500 and 3 μm catalyst) which indicates the significant influence of the co-catalyst on catalytic activity in transition metal-catalysed ethylene oligomerization. Enhancing the Al/Cr ratio up to 900, led to decreasing the productivity because MMAO acts as poison at higher aluminium alkyl concentrations (e.g., Al/Cr = 900 and 3 μm catalyst).

As shown in Fig. 3b, increasing the Al/Cr ratio up to 900 (at a constant ethylene pressure of 15 bar), leads to enhanced 1- C_6 productivity as well as transition metal activation. Furthermore, at higher ethylene pressure of 27 bar (for Al/Cr ratio between 500 and 900), the catalyst (7) showed relatively high activity due to the greater catalyst stability and higher ethylene solubility under higher ethylene pressures.

Figure 3c shows the interaction of temperature with the Al/Cr ratio. In general, the suitable active sites were formed at elevated temperature up to 80 $^\circ\text{C}$ and 1- C_6 productivity

increased. The activity decreased with a further increase in temperature due to the deactivation of the catalyst. Further experiments at elevated temperatures such as 90, 100 and 120 $^\circ\text{C}$, showed a great reduction toward 1- C_6 production. The thermal analysis results also confirmed the decomposition of the catalyst at high temperatures.

According to the Fig. 3d, with increasing the catalyst concentration the 1-hexene productivity increases. Figure 3e further confirms that temperature plays a key role in the catalyst productivity. It should also be noted that increasing the catalyst concentration at a constant temperature of 25 $^\circ\text{C}$ does not have an impact on productivity. Increasing the temperature resulted in a significant increase in 1- C_6 productivity (for catalyst concentration from 3 to 9 μm).

As presented in Fig. 3f, increasing the ethylene pressure at a constant temperature of 25 $^\circ\text{C}$ does not show any positive influence on the productivity. Our studies have identified low temperatures which could be limiting the ethylene reaction and hence negatively affect the yields.

Figure 4 also indicates the 1- C_6 productivity (the response) versus those of the empirical model. The predicted data of the response from the empirical model agreed well with the observed ones in the range of the operating variables. The model predicted the optimal values of the four variables; Al/Cr: 841, catalyst concentration: 8.7 μmol , temperature: 58.2 $^\circ\text{C}$, ethylene pressure: 19.5 bar corresponding to $\ln(\text{productivity } 1\text{-}C_6) = 10.6 \text{ g } 1\text{-}C_6/\text{g Cr h}$. The statistical optimization used in this research showed the higher 1- C_6 productivity comparing with other results on the ethylene trimerization using pyridine-based catalyst [29].

A generalized mechanism for activation by co-catalyst and ethylene oligomerization via metallacycle intermediates is shown in Scheme 2. Among the several transition elements in different oxidation states that show catalytic activity in terms of ethylene oligomerization, trivalent chromium appears to be the most versatile species. Trivalent chromium has produced the best performing trimerization and tetramerization catalysts in terms of both activity and selectivity and accounts for over 90% of all the existing oligomerization catalysts. The oxidation state of chromium(III) was previously confirmed by using UV-Vis spectra for all synthesized catalysts. The process begins with oxidative (with respect to the metal) coupling of two ethylene units to produce a metallacyclopentane complex. From here, insertion of further ethylene into the metallacyclopentane produces larger ring metallacycles, while breakdown of the metallacycle at any point can produce linear α -olefins. Thus the selectivity of the process is controlled by the relative stability of the different sized metallacycles, in particular their tendency to either decompose or grow via ethylene insertion. For selective ethylene trimerization, release of 1-hexene is fast inhibiting further ring growth and thus formation of higher α -olefins [9, 37].

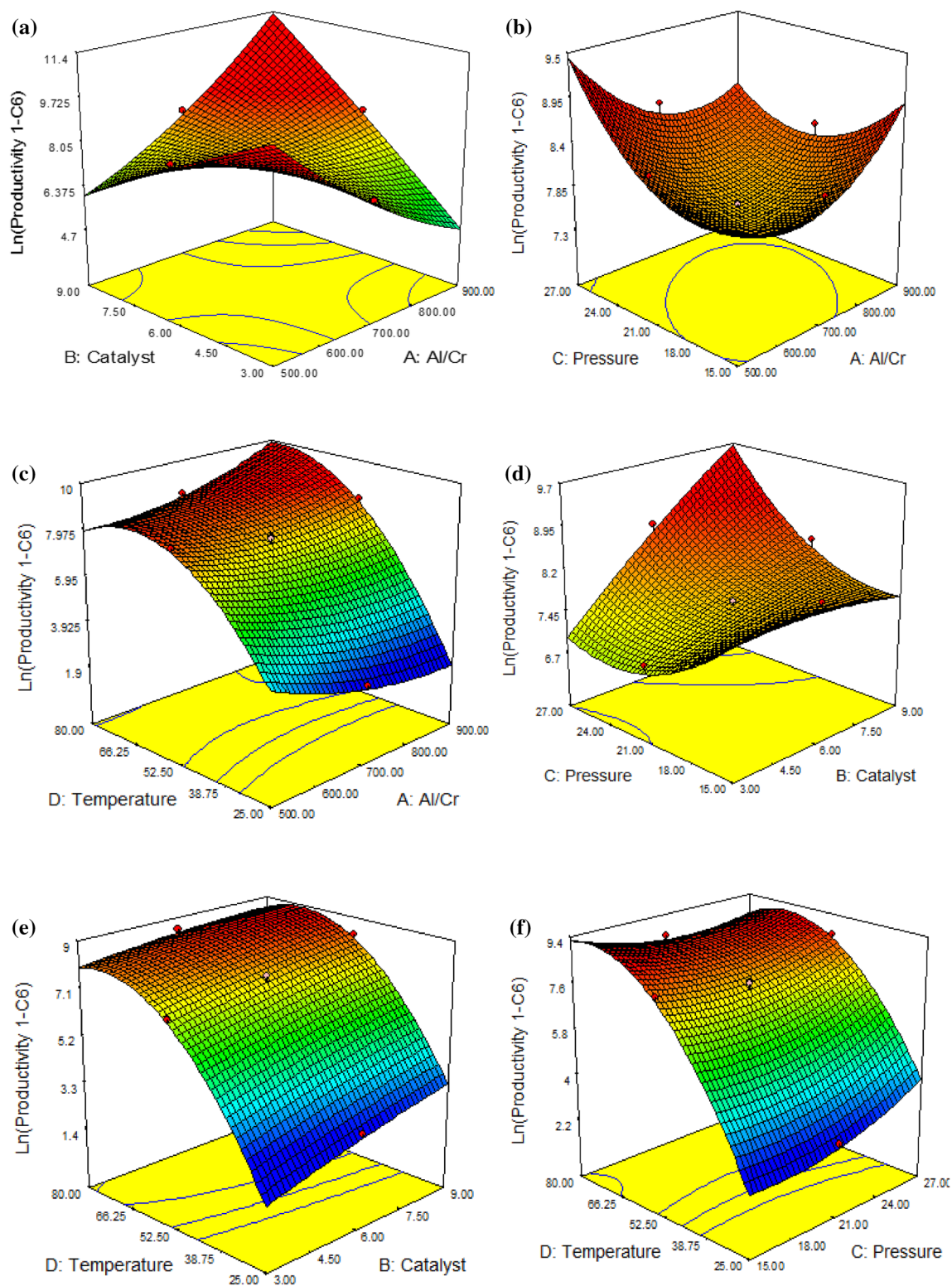


Fig. 3 The interaction effect among various effective parameters on 1-C₆ productivity

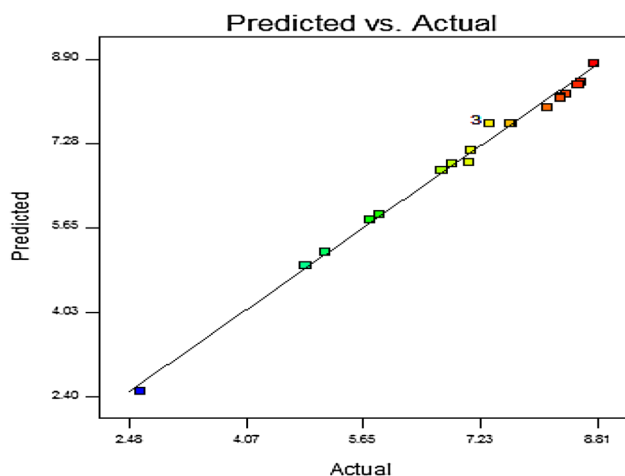


Fig. 4 The predicted values by the model against the actual values

Yang et al. theoretically studied a mechanism for ethylene trimerization catalyzed by $\text{MeS}(\text{CH}_2)_2\text{N}(\text{H})(\text{CH}_2)_2\text{SMe-Cr}(\text{I})$ catalyst and calculated the Gibbs free energy for different intermediates. Their results confirmed that metallacycloheptane are important intermediate responsible for ethylene trimerization into 1-hexene [38].

As shown in Table 7, the quantity of polyethylene produced in the ethylene reaction catalyzed by pyridine-based catalyst was measured for several runs. Unexpectedly a switching from ethylene trimerization to polymerization occurred by exchanging of the ethylene pressure (Table 7, Runs 8 and 10) that has not been reported yet. The above propose mechanism (Scheme 2) can justify this phenomenon. For this specific reaction condition, low release of 1- C_6 and further ring growth lead to the formation of polyethylene according to the extended metallacycle mechanism at higher ethylene pressure [9]. Moreover, for the formation of polymer during the of ethylene oligomerization process, a mechanism similar to the mechanism for Phillips catalyst polymerization can be imagined. Three

Scheme 2 Proposed metallacycle mechanism for production of 1-hexene, 1-Octene, higher LAOs and polyethylene using chromium catalysts bearing pyridine based SNS ligands

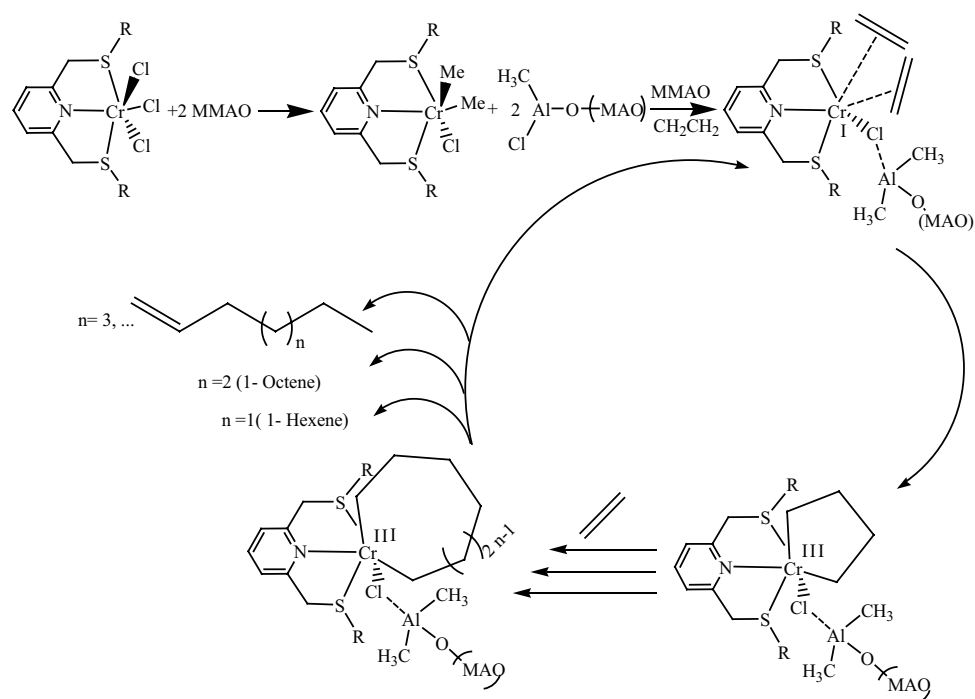


Table 7 Comparison between the quantities of polyethylene produced in the ethylene reaction catalyzed by pyridine-based catalyst (7) for several runs

Run	A: Al/Cr	B: Catalyst (μmol)	C: Ethylene pressure (bar)	D: Temperature ($^{\circ}\text{C}$)	Weight of PE (g)	Productivity (g PE/g Cr h)
1	700	6	21	52.5	0.15	961
8	900	3	27	80	7.90	101282 ^a
10	900	3	15	80	0.02	262
19	700	6	27	52.5	0.10	614

^aMaximum PE productivity using catalyst (7) obtained by change the ethylene pressure

kinds of typical initiation mechanisms have been proposed in the literatures for the Phillips chromium catalyst: Cossee mechanism, carbene mechanism, and metallacycle mechanism. However, these mechanisms do not definitely justify the polymer formation during the Phillips polymerization process [39, 40].

It is, highly desirable to find the reasons that are responsible for the formation of polymeric materials. So DSC was used to study the thermal properties of the resulting polyethylenes (Table 7, Runs 8 and 10, Fig. 6). The samples were heated from 25 to 180 °C, held for 1 min to erase thermal history effects and cooled to 25 °C and then heated to 180 °C again for the second scan. The temperature scan was performed with a heating and cooling rate of 10 °C/min. As shown in Fig. S2 the DSC curve of the polymer (Run 8) show an exothermic peak at 135 °C ($\Delta H = 170$ J/g) which is a typical DSC endotherms of polyethylene with different molecular weight. Also, no difference was observed in the cooling and second heating cycles (Table S1). The first heating scan provides information about the thermal history of the sample (processing or aging). The cooling and second heating cycles are then performed at known thermal history. The similar melting point of the sample (Run 8) in second heating cycle shows that the processing conditions did not have any effect on the thermal properties of the polyethylene. But the polyethylene sample produced as

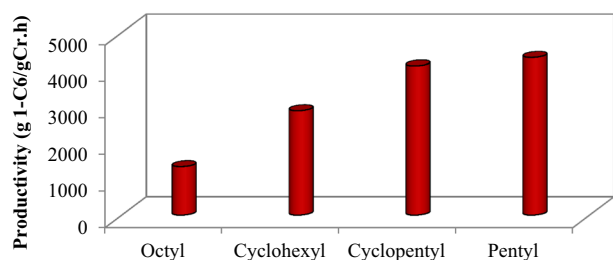
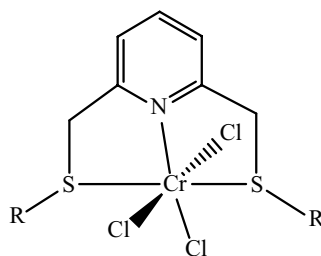
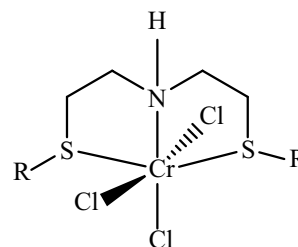


Fig. 5 Comparison of various pyridine-based catalysts with different substituent on sulphur atom (temperature: 52.5 °C, catalyst concentration: 6 μmol, ethylene pressure: 27 bar, Al/Cr: 500, solvent: toluene)

Fig. 6 Comparison of pyridine-SNS-alkyl/CrCl₃ and amine-SNS-alkyl/CrCl₃ catalysts in ethylene trimerization



Pyridine-SNS/Catalyst
Selectivity: > 99%
Productivity: 6420 (g 1-C₆/gr Cr. h)



Amine-SNS/Catalyst
Selectivity: > 99%
Productivity: 141*10³ (g 1-C₆/gr Cr. h)

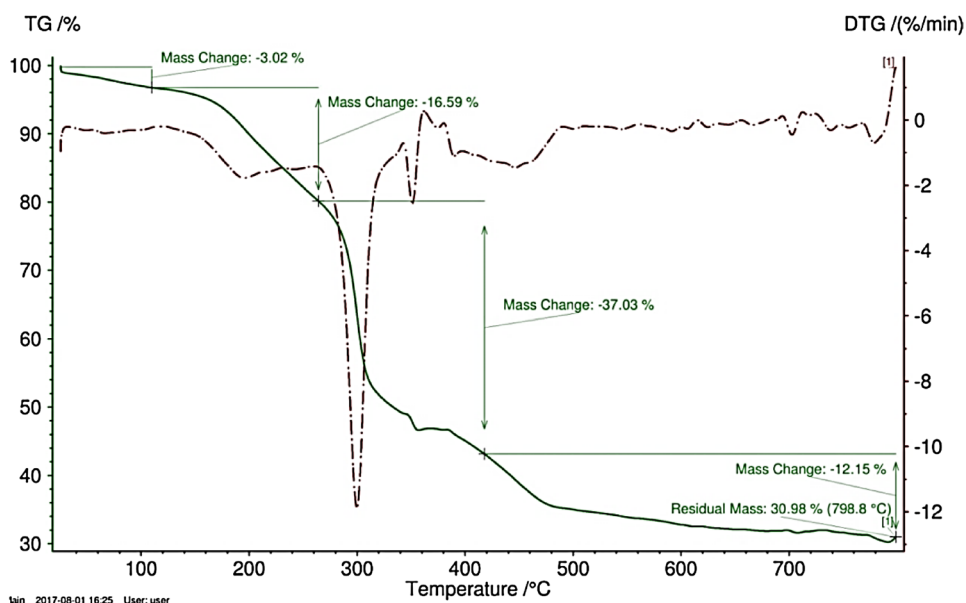
by-product in Run 10 had significantly lower T_m (134 °C) and melting enthalpy (ΔH_m) values may be due to the degradation and decreasing the size of crystals. The polymer sample (Run 10) contains chains with a wide distribution of chain lengths and shows the low crystallinity (%). Oligomers with low molecular weight may be the main reason of the lower X_c (%) observed for the obtained polyethylene (Table S1, Run 10).

Selected ethylene trimerization results of different pyridine-based catalysts were also investigated. According to Fig. 5, it is clear that the pyridine-SNS-alkyl-CrCl₃ systems are capable to production of 1-C₆ with more than 90% selectivity, which highlights them among other available catalytic systems. The substituents on the sulphur atom have great influences on the catalytic performance. Increasing the size of substituents rises the steric bulk around the S (steric hindrance). So further insertion of ethylene into the chromacyclopentane ring significantly restricts.

3.5 Ethylene Trimerization Using Amine-SNS-Alkyl/CrCl₃ Catalysts

Amine-SNS-Alkyl/CrCl₃ catalysts similar to pyridine-based catalysts have also been effective for selective ethylene trimerization. In addition, intensely lower cost of the SNS ligands, small amount of expensive MMAO, improved activity (141,000 g/g Cr h) (Table S2) retaining high 1-C₆ selectivity make them superior in terms of potential technical application. Similar to the trend observed for the pyridine-based complexes, increasing the steric hindrance on side chain leads to lower catalytic activities, while the opposite effect is observed as the steric hindrance decreases. In addition to R-group steric difference as a determining factor of catalytic activity in the prepared complexes, the amine N-donor containing complexes (**14–16**) displayed a significantly higher catalytic activity which is likely due to the additional flexibility of the amine backbone. A flexible two carbon spacer between a simple amine N donor and the S-donor atoms generated more effective catalysts than a rigid

Fig. 7 TGA diagram of amine-SNS-pentyl/CrCl₃ catalyst under nitrogen atmosphere and heating rate of 10 °C/min from ambient temperature up to 800 °C



pyridine N-donor linked to the S-donors via a methylene spacer. Direct comparison of the two structurally catalysts in Fig. 6 further confirmed the importance of the flexibility factor influence as a key factor of catalytic activity and more ethylene insertion as well as the metallacycloheptane ring formation. The thermogravimetric analysis (TGA) curves in nitrogen showed that the amine-based complexes display lower thermal stability compared to pyridine-based complexes (Fig. 7). The decomposition temperatures (T_{dec}) for 5% weight loss were observed in the range of 162 °C for amine-SNS-pentyl/CrCl₃. The initial weight loss (~3.23%) is related to the residual organic solvent and water. The second and the third weight loss (16.59%) in the temperature range of 120–220 °C, presumably due to loss of the NHC₄H₈ fragment of the SNS ligand. The fourth weight loss (49%) in the temperature range of 260–420 °C is related to the dissociation of the SC₅H₁₁ of the ligand. The residual mass (31%) above 800 °C can be assigned to CrCl₃. The presence of pyridine ring increases the thermal stability and degradation temperature of pyridine-base catalysts compared to amine-based catalysts.

4 Conclusions

Two types of chromium catalysts bearing pyridine and amine based SNS ligands were synthesized. Response surface methodology (RSM) based on a three level-four variable central composite design, was employed to evaluate the effect of the most important parameters on 1-C₆ productivity. The temperature was found as major influential factor on the 1-C₆ productivity. The experimental results indicated that there is reasonably good agreement between predictions

and experiments. A switching from ethylene trimerization to polymerization of the catalyst system can be occurred utilizing exchanging of the reaction conditions. The polymer produced as by-product of catalytic ethylene oligomerization using pyridine-based catalyst contains chains with a wide distribution of chain lengths and shows the low crystallinity. Increasing the steric hindrance on side chain leads to lower catalytic activities. Chromium catalysts based on amine ligands show higher 1-C₆ productivity. Comparison of the two structurally catalysts confirmed the importance of the flexibility factor influence as a key factor of catalytic activity and more ethylene insertion as well as the metallacycloheptane ring formation. The presence of pyridine ring increases the thermal stability and degradation temperature of pyridine-base catalysts compared to amine-based catalysts. The selectivity of these systems makes them very suitable for use in tandem with olefin polymerization catalysts to produce LLDPE from ethylene alone; results in this area will be reported shortly.

Acknowledgements The authors would like to thank Mr. Abbas Biglari for his sincere efforts to NMR analysis of the samples.

Funding The authors would like to thank the Iran National Science Foundation (INSF) for the financial support of this study (Grant Number 95824926) and from the Institute for Advanced Studies in Basic Sciences (IASBS) for its financial and spiritual supports.

Compliance with Ethical Standards

Conflict of interest There is no conflict of interest for each contributing authors.

References

- Liu S, Zhang Y, Han Y et al (2017) Selective ethylene oligomerization with chromium-based metal–organic framework MIL-100 evacuated under different temperatures. *Organometallics* 36(3):632–638
- Britovsek GJ, Malinowski R, McGuinness DS et al (2015) Ethylene oligomerization beyond Schulz–Flory distributions. *ACS Catal* 5(11):6922–6925
- Rozhko E, Bavykina A, Osadchii D et al (2017) Covalent organic frameworks as supports for a molecular Ni based ethylene oligomerization catalyst for the synthesis of long chain olefins. *J Catal* 345:270–280
- Vilms AI, Babenko IA, Bezborodov VA et al (2017) Ethylene oligomerization over chromium(III) complexes with pyrrole derivatives. *Petrol Chem* 57(3):244–250
- Mohamadnia Z, Ahmadi E, Haghghi MN et al (2015) Preparation of LLDPE through tandem ethylene polymerization using chromium and zirconium catalysts. *Iran Polym J* 24(8):621–628
- Fallahi M, Ahmadi E, Ramazani A et al (2017) Trimerization of ethylene catalyzed by Cr-based catalyst immobilized on the supported ionic liquid phase. *J Organomet Chem* 848:149–158
- Xu Z, Chada JP, Xu L, et al. (2018) Ethylene dimerization and oligomerization to 1-butene and higher olefins with chromium-promoted cobalt on carbon catalyst. *ACS Catal* 8(3):2488–2497
- Lappin GR, Nemeč LH, Sauer JD et al (2000) Olefins, higher. *Kirk-Othmer encyclopedia of chemical technology*. Wiley, New York
- McGuinness DS (2010) Olefin oligomerization via metallacycles: dimerization, trimerization, tetramerization, and beyond. *Chem Rev* 111(3):2321–2341
- Bergamo AL, Da Cas HK, Rambo RS et al (2016) Chromium complexes bearing pyrazolyl-imine-phenoxy/pyrrolide ligands: synthesis, characterization, and use in ethylene oligomerization. *Catal Commun* 86:77–81
- Kuhlmann S, Paetz C, Hägele C et al (2009) Chromium catalyzed tetramerization of ethylene in a continuous tube reactor—proof of concept and kinetic aspects. *J Catal* 262(1):83–91
- Reagan WK, Freeman JW, Conroy BK et al (1994) Phillips Petroleum Company, Bartlesville
- Tanaka E, Urata H, Oshiki T et al (2000) Process for producing alpha-olefin oligomer compositions. EP 0611743 B2. Mitsubishi Chemical Corporation
- Carter A, Cohen SA, Cooley NA et al (2002) High activity ethylene trimerisation catalysts based on diphosphine ligands. *Chem Commun* 8:858–859
- Bollmann A, Blann K, Dixon JT et al (2004) Ethylene tetramerization: a new route to produce 1-octene in exceptionally high selectivities. *J Am Chem Soc* 126(45):14712–14713
- Hao Z, Xu B, Gao W (2015) Chromium complexes with N, N, N-tridentate quinolinyl anilido-imine ligand: synthesis, characterization, and catalysis in ethylene polymerization. *Organometallics* 34(12):2783–2790
- Suttill JA, Wasserscheid P, McGuinness DS et al (2014) A survey of pendant donor-functionalised (N, O) phosphine ligands for Cr-catalysed ethylene tri- and tetramerisation. *Catal Sci Technol* 4(8):2574–2588
- Alzamly A, Gambarotta S, Korobkov I (2013) Synthesis, structures, and ethylene oligomerization activity of bis (phosphanylamine) pyridine chromium/aluminate complexes. *Organometallics* 32(23):7107–7115
- Ahmadi E, Mohamadnia Z, Haghghi MN (2011) High productive ethylene trimerization catalyst based on CrCl₃/SNS ligands. *Catal Lett* 141(8):1191
- Albahily K, Shaikh Y, Ahmed Z et al (2011) Isolation of a self-activating ethylene trimerization catalyst of a Cr-SNS system. *Organometallics* 30(15):4159–4164
- Mohamadnia Z, Ahmadi E, Haghghi MN et al (2011) Synthesis and optimization of ethylene trimerization using [bis-(2-dodecylsulfanyl-ethyl)-amine] CrCl₃ catalyst. *Catal Lett* 141(3):474–480
- Yang Y, Liu Z, Liu B et al (2013) Selective ethylene tri-/tetramerization by in situ-formed chromium catalysts stabilized by N,P-based ancillary ligand systems. *ACS Catal* 3(10):2353–2361
- Yang Y, Gurnham J, Liu B et al (2014) Selective ethylene oligomerization with chromium complexes bearing pyridine–phosphine ligands: influence of ligand structure on catalytic behavior. *Organometallics* 33(20):5749–5757
- Zhang J, Braunstein P, Hor TA (2008) Highly selective chromium (III) ethylene trimerization catalysts with [NON] and [NSN] heteroscorpionate ligands. *Organometallics* 27(17):4277–4279
- Liu S, Pattacini R, Braunstein P (2011) Reactions between an ethylene oligomerization chromium(III) precatalyst and aluminum-based activators: alkyl and cationic complexes with a tridentate NPN ligand. *Organometallics* 30(13):3549–3558
- Simler T, Braunstein P, Danopoulos AA (2016) Chromium(II) pincer complexes with dearomatized PNP and PNC ligands: a comparative study of their catalytic ethylene oligomerization activity. *Organometallics* 35(24):4044–4049
- Jie S, Pattacini R, Rogez G et al (2009) Synthesis, structure, magnetic and catalytic properties of new dinuclear chromium(III) complexes with oxazoline alcoholate ligands. *Dalton Trans* 1:97–105
- Ai P, Danopoulos AA, Braunstein P (2015) N-Phosphanyl and N,N'-diphosphanyl-substituted N-heterocyclic carbene chromium complexes: synthesis, structures, and catalytic ethylene oligomerization. *Organometallics* 34(16):4109–4116
- Temple CN, Gambarotta S, Korobkov I et al (2007) New insight into the role of the metal oxidation state in controlling the selectivity of the Cr-(SNS) ethylene trimerization catalyst. *Organometallics* 26(18):4598–4603
- McGuinness DS, Wasserscheid P, Keim W et al. (2003) First Cr (III)—SNS complexes and their use as highly efficient catalysts for the trimerization of ethylene to 1-hexene. *J Am Chem Soc* 125(18):5272–5273
- Komarsamy L, Bala MD, Friedrich HB et al (2011) 2,6-Bis(tosyl-oxymethyl)pyridine. *Acta Crystallogr E* 67:302
- Soobramoney L, Bala MD, Friedrich HB (2014) Coordination chemistry of Co complexes containing tridentate SNS ligands and their application as catalysts for the oxidation of n-octane. *Dalton Trans* 43(42):15968–15978
- Dixon JT, Green MJ, Hess FM et al (2004) Advances in selective ethylene trimerisation—a critical overview. *J Organomet Chem* 689(23):3641–3668
- Núñez-Dallos N, Lopez-Barbosa N, Muñoz-Castro A et al (2017) A new copper (I) coordination polymer from 2, 6-bis (1*H*-benzotriazol-1-ylmethyl)pyridine: Synthesis, characterization, and use as additive in transparent submicron UV filters. *J Coord Chem* 70(19):3363–3378
- Janse van Rensburg W, van den Berg JA, Steynberg PJ (2007) Role of MAO in chromium-catalyzed ethylene tri- and tetramerization: a DFT study. *Organometallics* 26(4):1000–1013
- García-Muñoz RA, Morales V, Linares M et al (2014) Influence of the structural and textural properties of ordered mesoporous materials and hierarchical zeolitic supports on the controlled release of methylprednisolone hemisuccinate. *J Mater Chem B* 2(45):7996–8004

37. Elowe PR, McCann C, Pringle PG et al (2006) Nitrogen-linked diphosphine ligands with ethers attached to nitrogen for chromium-catalyzed ethylene tri- and tetramerizations. *Organometallics* 25(22):5255–5260
38. Yang Y, Liu Z, Zhong L et al (2011) Spin surface crossing between chromium (I)/sextet and chromium (III)/quartet without deprotonation in SNS-Cr mediated ethylene trimerization. *Organometallics* 30(19):5297–5302
39. Gandon V, Agenet N, Vollhardt KP et al (2006) Cobalt-mediated cyclic and linear 2:1 co-oligomerization of alkynes with alkenes: a DFT study. *J Am Chem Soc* 128(26):8509–8520
40. Ghiotti G, Garrone E, Zecchina A (1991) An infrared study of CO/C₂H₄ coadsorption and reaction on silica-supported Cr(II) ions. *J Mol Catal* 65(1–2):73–83

Affiliations

Majid Soheili¹  · Zahra Mohamadnia¹  · Babak Karimi¹ 

✉ Zahra Mohamadnia
z.mohamadnia@iasbs.ac.ir

¹ Department of Chemistry, Institute for Advanced Studies in Basic Sciences (IASBS), No. 444, Prof. Yousef Sobouti Blvd., P. O. Box 45195-1159, Zanjan 45137-66731, Iran